The Astrophysical Journal, 808:175 (7pp), 2015 August 1 doi:10.1088/0004-637X/808/2/175

BROADENING OF H_2O ROTATIONAL LINES BY COLLISIONS WITH He ATOMS AT LOW TEMPERATURE

M. I. Hernández[1], J. M. Fernández[2], G. Tejeda[2], E. Moreno[2], and S. Montero[2]
[1] Instituto de Física Fundamental CSIC, Serrano 123, E-28006 Madrid, Spain
[2] Laboratory of Molecular Fluid Dynamics, Instituto de Estructura de la Materia CSIC, Serrano 121, E-28006 Madrid, Spain; jm.fernandez@csic.es
Received 2015 April 22; accepted 2015 June 17; published 2015 July 30

ABSTRACT

We report pressure broadening (PB) coefficients for the 21 electric–dipole transitions between the eight lowest rotational levels of ortho-H_2O and para-H_2O molecules by collisions with He at temperatures from 20 to 120 K. These coefficients are derived from recently published experimental state-to-state rate coefficients for H_2O:He inelastic collisions, plus an elastic contribution from close coupling calculations. The resulting coefficients are compared to the available experimental data. Mostly due to the elastic contribution, the PB-coefficients differ much from line to line, and increase markedly at low temperature. The present results are meant as a guide for future experiments and astrophysical observations.

Key words: astronomical databases: miscellaneous – ISM: lines and bands – ISM: molecules – methods: laboratory: molecular – molecular data – submillimeter: general

1. INTRODUCTION

Pressure broadening (PB) of spectral lines is useful for remote sensing in astrophysics, allowing for a straightforward determination of the number density of colliders. Since H_2O is a relevant observational target in present day astrophysics (van Dishoeck et al. 2013), we focus the discussion below on this species, in particular on the broadening induced by collisions with He atoms. Microwave measurements of pressure broadening coefficients (PB-coefficients in short) of rotational lines of H_2O by collisions with He at low temperature have been reported by Goyette & de Lucia (1990), Dutta et al. (1993), and Dick et al. (2010). However, these experiments pose severe difficulties due to the strong tendency of gaseous water to condense, and are limited to the few spectral lines within reach of the particular instrument.

On the other hand, PB-coefficients are often derived from the state-to-state rate coefficients (sts-rates in short) for inelastic collisions. We have recently published (Tejeda et al. 2015) a laboratory study of the rotational inelastic collisions of H_2O with He atoms at low temperature (20–120 K). In that work a new collection of experimentally derived sts-rates was reported, with 1σ uncertainty of $\approx$6% at 120 K and $\approx$11% at 20 K.

There is, however, a further contribution to the PB-coefficients due to interferences between elastic amplitudes, which can be relevant in some cases. Here, we have obtained this elastic term from close-coupling (CC) calculations, employing the potential energy surface (PES) by Patkowski et al. (2002). The relative importance of the elastic and inelastic contributions to the broadening of H_2O spectral lines by helium is assessed.

The main goal of the present work is to provide an extended set of PB-coefficients for H_2O lines by collisions with He, based on the experimental sts-rates. This set includes most transitions observed in the Water In Star-forming Regions with Herschel program (van Dishoeck et al. 2011). These PB-coefficients, which are a sum of inelastic and elastic contributions from experiments and theory, respectively, allow us to review the PB-coefficients published so far.

2. THEORETICAL FRAME FOR THE PB OF SPECTRAL LINES

At densities low enough to prevent strong line mixing, the Lorentzian half-width at half-maximum Γ_{if} of an $i \rightarrow f$ spectral line is given by

$$\Gamma_{if} = \gamma_{if}\, p, \tag{1}$$

where p is the total pressure of colliders and γ_{if} is the PB-coefficient, which depends only on the translational temperature T of the bath and on the nature of the colliders; γ_{if} can be expressed in terms of a thermally averaged PB cross section $\sigma_{if}(T)$ (PBx-sections in short) as

$$\gamma_{if}(T) = \frac{1}{2\pi}\frac{1}{k_{\rm B}T}\, v\, \sigma_{if}(T), \tag{2}$$

where $k_{\rm B}$ is Boltzmann constant, and $v = \sqrt{(8k_{\rm B}T)/(\pi\mu)}$ is the mean relative velocity of colliding partners of a reduced mass μ.

The PBx-section is usually given as a sum of two contributions (Baranger 1958; Wiesenfeld & Faure 2010)

$$\sigma_{if}(T) = \sigma_{if}^{(\rm in)}(T) + \sigma_{if}^{(\rm el)}(T), \tag{3}$$

one inelastic, $\sigma_{if}^{(\rm in)}(T)$, and another elastic, $\sigma_{if}^{(\rm el)}(T)$. The inelastic contribution can be calculated in favorable cases from the sts-rates $k_{i\rightarrow j}(T)$ for inelastic collisions, tabulated in databases like BASECOL (Dubernet et al. 2013) or LAMDA (Schöier et al. 2005), by means of

$$\sigma_{if}^{(\rm in)}(T) = \frac{1}{2v}\left[\sum_{j\neq i} k_{i\rightarrow j}(T) + \sum_{j\neq f} k_{f\rightarrow j}(T)\right]. \tag{4}$$

On the other hand, the elastic contribution,

$$\sigma_{if}^{(\rm el)}(T) = \left\langle \int d\Omega |f_i(\Omega, E_{\rm k}) - f_f(\Omega, E_{\rm k})|^2 \right\rangle_T, \tag{5}$$

is due to the interference between the elastic scattering amplitudes f_i and f_f for the two states involved in the transition (Baranger 1958; Wiesenfeld & Faure 2010), which are

Table 1
Identification of Rotational Energy Levels of $H_2^{16}O$ in the Vibrational Ground State, after Tennyson et al. (2001)

Para-H_2O					Ortho-H_2O				
i	E_i (cm^{-1})	J	K_a	K_c	i	E_i (cm^{-1})	J	K_a	K_c
1	0.0000	0	0	0	1	23.7944	1	0	1
2	37.1371	1	1	1	2	42.3717	1	1	0
3	70.0908	2	0	2	3	79.4964	2	1	2
4	95.1759	2	1	1	4	134.9016	2	2	1
5	136.1639	2	2	0	5	136.7617	3	0	3
6	142.2785	3	1	3	6	173.3658	3	1	2
7	206.3014	3	2	2	7	212.1564	3	2	1
8	222.0527	4	0	4	8	224.8384	4	1	4

functions of the scattering angle, Ω, and of the kinetic energy, E_k, while $\langle\ \rangle_T$ indicates a thermal average. This contribution $\sigma_{if}^{(el)}(T)$, which includes both reorientation and dephasing effects, cannot be derived straightforwardly neither from tabulated material nor from experiment. However, it can be calculated through advanced quantum methods like the CC approach, along with a good PES for the colliding pair.

In the rigid rotor approximation, the elastic contribution $\sigma_{if}^{(el)}(T)$ to the PBx-section is strictly zero for the isotropic part of the Q-branch ($\Delta J = 0$) lines in the vibrational Raman spectra. The so-called random phase approximation (RPA; DePristo & Rabitz 1979) assumes extending the vanishing of $\sigma_{if}^{(el)}(T)$ to the electric–dipole or quadrupole absorption/emission lines in the infrared and microwave regions. This can be explained in part because of the convenience of Equation (4) and the availability of the required data, and also because the RPA has proven to be a reasonable approximation for a number of small molecules (Green 1980, 1989; Palma & Green 1986; Thibault et al. 2000, 2002, 2009). For asymmetric top molecules, however, the elastic contribution has been shown to be important at least for the PB of H_2O rotational lines by H_2 at low temperature (Wiesenfeld & Faure 2010; Drouin & Wiesenfeld 2012; Faure et al. 2013). The extent of elastic and inelastic contributions to the PB of H_2O rotational lines by He is discussed below.

3. PROCEDURE AND RESULTS

Labels i for the rotational energy levels of para-H_2O and ortho-H_2O relevant for the present work are given in Table 1. Experimental PB-coefficients γ_{if} for just eight rotational lines of H_2O have been reported so far by Goyette & de Lucia (1990), Dutta et al. (1993), and Dick et al. (2010) for collisions with He at low temperature. For an easier comparison with the calculations, it is convenient to transform them into the corresponding PBx-sections by means of Equation (2) expressed as

$$\sigma_{if} = 0.4472\ \sqrt{\mu T}\ \gamma_{if}, \tag{6}$$

where σ_{if} is in $Å^2$ for γ_{if} given in MHz $Torr^{-1}$, μ in amu, and T in K. The above quoted experimental data are plotted in Figure 1 as bullet symbols, where the data from Dick et al. (2010) are referred to the temperature calibration $T_{gas} = 0.8849\ T_{cell} + 41.62$. A preliminary interpretation of the PB-data by Dick et al. (2010) was attempted by these authors within the RPA, i.e., neglecting in Equation (3) the elastic contribution to the PBx-section, and using Equation (4) with the sts-rates calculated by Green et al. (1993). These sts-rates have been shown to be significantly smaller than the experimental ones by Tejeda et al. (2015), and also smaller than those calculated by Yang et al. (2013), employing the improved H_2O–He PES by Patkowski et al. (2002). Although Dick et al. (2010) attained a reasonable agreement between theory and experiment for the six lines over 500 GHz, we noticed that such interpretation, neglecting $\sigma_{if}^{(el)}$, sharply disagrees for the $5 \rightarrow 6$ (183 GHz) line of para-H_2O by Goyette & de Lucia (1990) and for the $7 \rightarrow 8$ (380 GHz) line of ortho-H_2O by Dutta et al. (1993; see Figure 1, top panels). This led us to suspect that the elastic contribution might be significant for the PB of H_2O lines by He.

In order to confirm or to refute the above conjecture, we have proceeded as follows. First, referring to Equation (3), we have calculated $\sigma_{if}^{(in)}(T)$ for the H_2O lines according to Equation (4) using the experimental sts-rates for H_2O:He inelastic collisions by Tejeda et al. (2015). These $\sigma_{if}^{(in)}(T)$ are plotted in Figure 1 as open rhombs. Then, for the elastic contribution $\sigma_{if}^{(el)CC}(T)$ we have carried out CC calculations with the MOLSCAT code (Hutson & Green 1994) based on the PES by Patkowski et al. (2002), which provides the best agreement with the experimental sts-rates for inelastic collisions (Tejeda et al. 2015). Details about the calculations are given in the Appendix.

The total PBx-sections, plotted in Figure 1 as black stars, are a sum

$$\sigma_{if}^{TOTAL}(T) = \sigma_{if}^{(in)}(T) + \sigma_{if}^{(el)CC}(T), \tag{7}$$

of an experimental inelastic term plus a calculated elastic one. They show a better agreement with the apparently anomalous experimental PBx-sections of the $5 \rightarrow 6$ (183 GHz) line of para-H_2O and the $7 \rightarrow 8$ (380 GHz) line of ortho-H_2O. The difference (stars minus open rhombs) clearly shows that, at low temperature, the elastic contribution to the total PBx-section is larger than the inelastic one for these two lines.

In view of the above results, we have extended the described procedure to a number of rotational lines suitable for astrophysical diagnostics of H_2O densities in media dominated by collisions with helium. PBx-sections σ_{if} and coefficients γ_{if}, both inelastic-only and total, for the 21 microwave lines between the eight lowest rotational levels of para-H_2O and ortho-H_2O due to collisions with He, are reported in Table 2 for six temperatures between 20 and 120 K.

4. DISCUSSION

First, we discuss the inelastic contribution, then the elastic one, and finally the total PBx-sections of H_2O by helium in the 20–120 K thermal range.

The inelastic contribution to the thermally averaged PBx-section of most lines reported in Figure 1 and Table 2 show a similar pattern. They range from 4 to 8 $Å^2$ for temperatures $20 \leqslant T \leqslant 120$ K, showing a shallow minimum at $T \simeq 40$ K, and lying, for a given T, within ± 1 $Å^2$ from the average, reaching an almost constant value of 7.4 $Å^2$ at 120 K. Exceptions to this pattern are the lines at 557 and 1113 GHz involving the lowest energy levels ($1 \rightarrow 2$) of para-H_2O and ortho-H_2O, whose inelastic contribution to the PBx-section decreases monotonically with the temperature down to

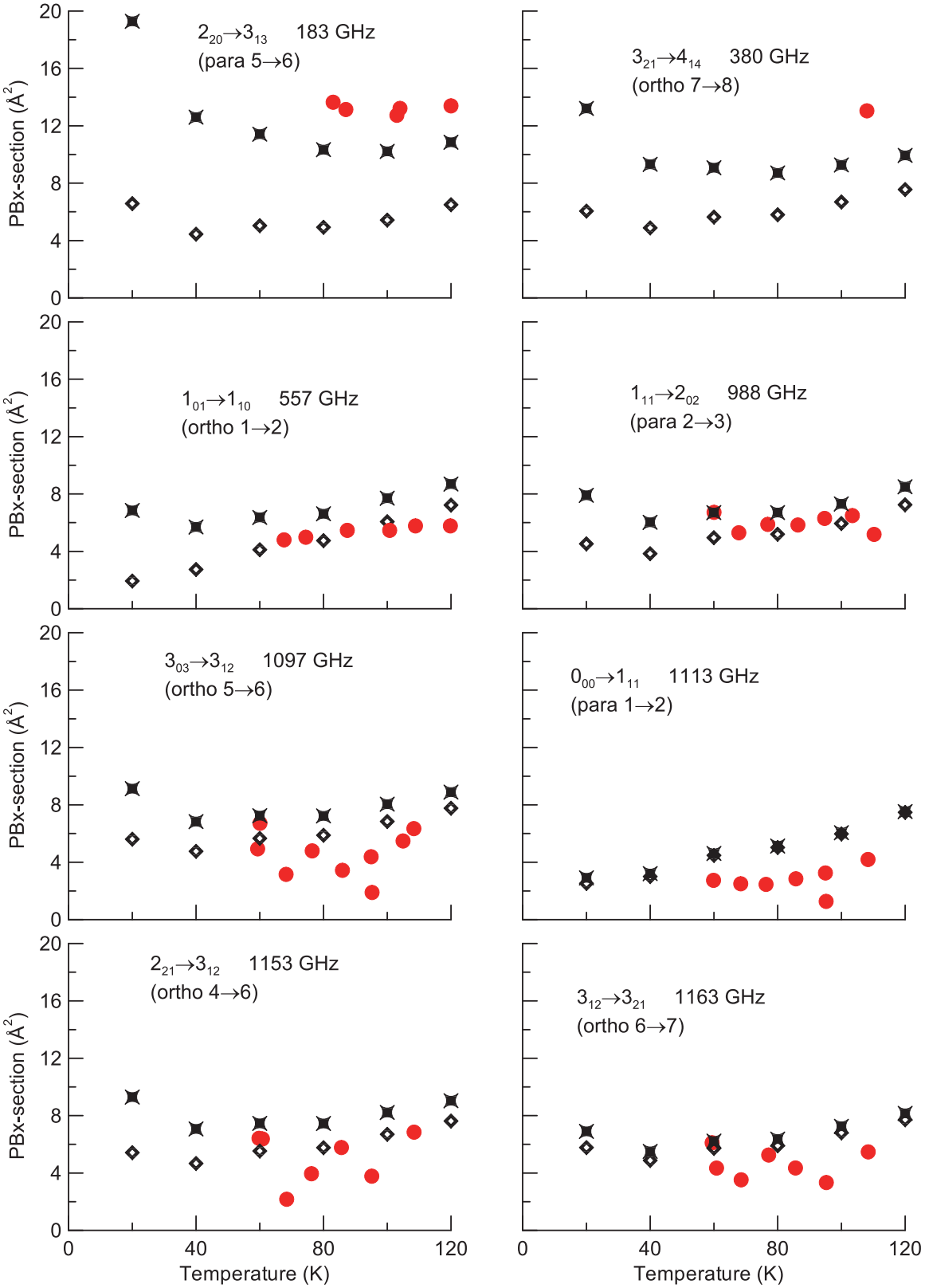

Figure 1. Experimental (bullets), inelastic (open rhombs), and total (stars) PBx-sections for some rotational lines of H_2O by collisions with He.

$\sigma_{if}^{(\mathrm{in})} < 3$ Å^2 at 20 K. This behavior can be rationalized as a statistical effect, since the number of available inelastic excitation and relaxation channels increases much with rotational energy for an asymmetric top molecule, and thus the summations of sts-rates in Equation (4) tend to average. The two exceptions are the $(1 \rightarrow 2)$ lines involving the ground states of each species, which can only be inelastically excited, in addition to the lower density of available states.

Table 2
Pressure Broadening Cross Sections σ_{if}, and Coefficients γ_{if}, for Rotational Lines of H_2O

						Inelastic		Total		Fit			
o/p	i	f	ω	ν	T	σ_{if}	γ_{if}	σ_{if}	γ_{if}	g	a	$b \times 10^5$	c
Para	5	6	183	6.1	20	6.58	1.817	19.29	5.330	1.120	1349.6	9.0712	115.89
	⋯	⋯	⋯	⋯	40	4.44	0.868	12.61	2.463	⋯	⋯	⋯	⋯
	⋯	⋯	⋯	⋯	60	5.03	0.803	11.42	1.822	⋯	⋯	⋯	⋯
	⋯	⋯	⋯	⋯	80	4.93	0.681	10.34	1.428	⋯	⋯	⋯	⋯
	⋯	⋯	⋯	⋯	100	5.43	0.671	10.22	1.263	⋯	⋯	⋯	⋯
	⋯	⋯	⋯	⋯	120	6.50	0.733	10.86	1.225	⋯	⋯	⋯	⋯
Ortho	7	8	380	12.7	20	6.06	1.674	13.21	3.649	1.051	884.60	4.8595	109.02
	⋯	⋯	⋯	⋯	40	4.89	0.955	9.31	1.820	⋯	⋯	⋯	⋯
	⋯	⋯	⋯	⋯	60	5.64	0.900	9.08	1.448	⋯	⋯	⋯	⋯
	⋯	⋯	⋯	⋯	80	5.80	0.802	8.71	1.204	⋯	⋯	⋯	⋯
	⋯	⋯	⋯	⋯	100	6.68	0.826	9.27	1.146	⋯	⋯	⋯	⋯
	⋯	⋯	⋯	⋯	120	7.56	0.853	9.94	1.121	⋯	⋯	⋯	⋯
Ortho	1	2	557	18.6	20	1.93	0.534	6.85	1.893	0.872	393.59	2.2416	60.12
	⋯	⋯	⋯	⋯	40	2.73	0.534	5.69	1.112	⋯	⋯	⋯	⋯
	⋯	⋯	⋯	⋯	60	4.12	0.657	6.36	1.015	⋯	⋯	⋯	⋯
	⋯	⋯	⋯	⋯	80	4.75	0.656	6.62	0.914	⋯	⋯	⋯	⋯
	⋯	⋯	⋯	⋯	100	6.07	0.750	7.70	0.952	⋯	⋯	⋯	⋯
	⋯	⋯	⋯	⋯	120	7.23	0.816	8.70	0.981	⋯	⋯	⋯	⋯
Para	3	4	752	25.1	20	6.28	1.736	10.42	2.879	0.891	703.16	3.6962	98.34
	⋯	⋯	⋯	⋯	40	4.65	0.909	7.29	1.425	⋯	⋯	⋯	⋯
	⋯	⋯	⋯	⋯	60	5.45	0.870	7.52	1.200	⋯	⋯	⋯	⋯
	⋯	⋯	⋯	⋯	80	5.42	0.748	7.18	0.992	⋯	⋯	⋯	⋯
	⋯	⋯	⋯	⋯	100	6.00	0.741	7.58	0.936	⋯	⋯	⋯	⋯
	⋯	⋯	⋯	⋯	120	7.17	0.809	8.63	0.973	⋯	⋯	⋯	⋯
Para	2	3	988	33.0	20	4.52	1.249	7.91	2.186	0.868	496.42	2.2328	77.48
	⋯	⋯	⋯	⋯	40	3.84	0.750	6.03	1.179	⋯	⋯	⋯	⋯
	⋯	⋯	⋯	⋯	60	4.96	0.791	6.71	1.070	⋯	⋯	⋯	⋯
	⋯	⋯	⋯	⋯	80	5.19	0.717	6.71	0.927	⋯	⋯	⋯	⋯
	⋯	⋯	⋯	⋯	100	5.94	0.734	7.30	0.902	⋯	⋯	⋯	⋯
	⋯	⋯	⋯	⋯	120	7.25	0.817	8.50	0.959	⋯	⋯	⋯	⋯
Ortho	5	6	1097	36.6	20	5.60	1.548	9.13	2.523	0.934	595.92	2.1550	87.37
	⋯	⋯	⋯	⋯	40	4.76	0.930	6.83	1.335	⋯	⋯	⋯	⋯
	⋯	⋯	⋯	⋯	60	5.66	0.903	7.25	1.157	⋯	⋯	⋯	⋯
	⋯	⋯	⋯	⋯	80	5.89	0.813	7.24	1.000	⋯	⋯	⋯	⋯
	⋯	⋯	⋯	⋯	100	6.84	0.845	8.05	0.995	⋯	⋯	⋯	⋯
	⋯	⋯	⋯	⋯	120	7.77	0.876	8.89	1.003	⋯	⋯	⋯	⋯
Para	1	2	1113	37.1	20	2.52	0.697	2.91	0.805	0.595	79.01	1.6770	0.00
	⋯	⋯	⋯	⋯	40	3.00	0.587	3.21	0.627	⋯	⋯	⋯	⋯
	⋯	⋯	⋯	⋯	60	4.48	0.715	4.62	0.736	⋯	⋯	⋯	⋯
	⋯	⋯	⋯	⋯	80	5.03	0.695	5.13	0.709	⋯	⋯	⋯	⋯
	⋯	⋯	⋯	⋯	100	5.98	0.739	6.06	0.749	⋯	⋯	⋯	⋯
	⋯	⋯	⋯	⋯	120	7.48	0.843	7.53	0.850	⋯	⋯	⋯	⋯
Ortho	4	6	1153	38.5	20	5.41	1.496	9.29	2.568	0.958	588.76	2.4599	94.36
	⋯	⋯	⋯	⋯	40	4.67	0.912	7.07	1.381	⋯	⋯	⋯	⋯
	⋯	⋯	⋯	⋯	60	5.54	0.883	7.46	1.190	⋯	⋯	⋯	⋯
	⋯	⋯	⋯	⋯	80	5.77	0.797	7.45	1.029	⋯	⋯	⋯	⋯
	⋯	⋯	⋯	⋯	100	6.70	0.828	8.23	1.017	⋯	⋯	⋯	⋯
	⋯	⋯	⋯	⋯	120	7.62	0.859	9.04	1.020	⋯	⋯	⋯	⋯
Ortho	6	7	1163	38.8	20	5.77	1.595	6.90	1.907	0.828	428.22	1.0157	45.56
	⋯	⋯	⋯	⋯	40	4.87	0.952	5.50	1.075	⋯	⋯	⋯	⋯
	⋯	⋯	⋯	⋯	60	5.71	0.911	6.22	0.993	⋯	⋯	⋯	⋯
	⋯	⋯	⋯	⋯	80	5.90	0.815	6.36	0.879	⋯	⋯	⋯	⋯
	⋯	⋯	⋯	⋯	100	6.81	0.842	7.26	0.897	⋯	⋯	⋯	⋯
	⋯	⋯	⋯	⋯	120	7.71	0.870	8.16	0.920	⋯	⋯	⋯	⋯
Para	4	5	1229	41.0	20	7.02	1.940	10.45	2.888	0.842	733.26	3.3809	98.75
	⋯	⋯	⋯	⋯	40	4.86	0.949	7.09	1.385	⋯	⋯	⋯	⋯
	⋯	⋯	⋯	⋯	60	5.48	0.874	7.26	1.157	⋯	⋯	⋯	⋯
	⋯	⋯	⋯	⋯	80	5.32	0.735	6.85	0.946	⋯	⋯	⋯	⋯
	⋯	⋯	⋯	⋯	100	5.83	0.720	7.20	0.890	⋯	⋯	⋯	⋯
	⋯	⋯	⋯	⋯	120	6.93	0.782	8.19	0.924	⋯	⋯	⋯	⋯

Table 2
(Continued)

						Inelastic		Total		Fit			
o/p	i	f	ω	ν	T	σ_{if}	γ_{if}	σ_{if}	γ_{if}	g	a	$b \times 10^5$	c
Ortho	3	4	1661	55.4	20	6.18	1.708	14.12	3.900	1.157	910.21	5.6451	110.87
	…	…	…	…	40	5.11	0.998	10.21	1.994	…	…	…	…
	…	…	…	…	60	5.98	0.953	9.97	1.591	…	…	…	…
	…	…	…	…	80	6.19	0.855	9.59	1.325	…	…	…	…
	…	…	…	…	100	7.15	0.883	10.19	1.259	…	…	…	…
	…	…	…	…	120	8.09	0.913	10.88	1.227	…	…	…	…
Ortho	1	3	1670	55.7	20	3.90	1.077	7.00	1.935	0.898	408.53	1.5086	50.59
	…	…	…	…	40	3.84	0.751	5.82	1.137	…	…	…	…
	…	…	…	…	60	5.04	0.804	6.59	1.052	…	…	…	…
	…	…	…	…	80	5.53	0.764	6.85	0.947	…	…	…	…
	…	…	…	…	100	6.70	0.828	7.90	0.976	…	…	…	…
	…	…	…	…	120	7.78	0.878	8.89	1.003	…	…	…	…
Ortho	3	5	1717	57.3	20	6.37	1.760	7.64	2.110	0.910	473.19	1.1446	56.06
	…	…	…	…	40	5.20	1.017	6.08	1.187	…	…	…	…
	…	…	…	…	60	6.10	0.973	6.82	1.088	…	…	…	…
	…	…	…	…	80	6.31	0.872	6.96	0.961	…	…	…	…
…	…	…	…	…	100	7.29	0.901	7.90	0.976	…	…	…	…
	…	…	…	…	120	8.24	0.930	8.83	0.996	…	…	…	…
Para	6	7	1919	64.0	20	6.86	1.894	11.17	3.085	0.846	808.88	3.4238	98.97
	…	…	…	…	40	4.62	0.903	7.37	1.440	…	…	…	…
	…	…	…	…	60	5.23	0.834	7.40	1.181	…	…	…	…
	…	…	…	…	80	5.12	0.708	6.98	0.964	…	…	…	…
	…	…	…	…	100	5.64	0.697	7.30	0.902	…	…	…	…
	…	…	…	…	120	6.74	0.760	8.27	0.933	…	…	…	…
Para	3	6	2164	72.2	20	5.84	1.613	7.33	2.026	0.731	498.66	1.7987	69.96
	…	…	…	…	40	4.24	0.828	5.26	1.028	…	…	…	…
	…	…	…	…	60	5.01	0.799	5.83	0.930	…	…	…	…
	…	…	…	…	80	5.02	0.694	5.72	0.791	…	…	…	…
	…	…	…	…	100	5.60	0.692	6.24	0.771	…	…	…	…
	…	…	…	…	120	6.74	0.761	7.33	0.827	…	…	…	…
Para	6	8	2392	79.8	20	6.48	1.792	7.39	2.043	0.670	539.11	1.4140	59.83
	…	…	…	…	40	4.41	0.861	5.01	0.980	…	…	…	…
	…	…	…	…	60	5.02	0.801	5.51	0.879	…	…	…	…
	…	…	…	…	80	4.93	0.681	5.36	0.740	…	…	…	…
	…	…	…	…	100	5.42	0.670	5.81	0.718	…	…	…	…
	…	…	…	…	120	6.50	0.734	6.87	0.775	…	…	…	…
Ortho	5	8	2640	88.1	20	5.88	1.626	6.77	1.872	0.795	429.17	0.9270	35.43
	…	…	…	…	40	4.77	0.933	5.34	1.043	…	…	…	…
	…	…	…	…	60	5.59	0.891	6.04	0.963	…	…	…	…
	…	…	…	…	80	5.79	0.800	6.18	0.853	…	…	…	…
	…	…	…	…	100	6.71	0.829	7.06	0.873	…	…	…	…
	…	…	…	…	120	7.62	0.859	7.95	0.897	…	…	…	…
Ortho	2	4	2774	92.5	20	4.22	1.165	7.63	2.107	0.900	453.09	2.2997	76.40
	…	…	…	…	40	4.00	0.781	6.12	1.196	…	…	…	…
	…	…	…	…	60	5.05	0.806	6.71	1.070	…	…	…	…
	…	…	…	…	80	5.41	0.747	6.82	0.942	…	…	…	…
	…	…	…	…	100	6.52	0.805	7.77	0.960	…	…	…	…
	…	…	…	…	120	7.54	0.850	8.67	0.978	…	…	…	…
Para	2	5	2969	99.0	20	5.26	1.453	9.79	2.704	0.858	675.83	3.1242	90.08
	…	…	…	…	40	4.05	0.791	6.80	1.329	…	…	…	…
	…	…	…	…	60	4.98	0.794	7.08	1.130	…	…	…	…
	…	…	…	…	80	5.10	0.704	6.86	0.947	…	…	…	…
	…	…	…	…	100	5.77	0.713	7.32	0.904	…	…	…	…
	…	…	…	…	120	7.01	0.790	8.41	0.948	…	…	…	…
Para	4	7	3331	111.1	20	7.30	2.017	7.67	2.120	0.725	546.10	1.5094	61.76
	…	…	…	…	40	5.03	0.984	5.31	1.038	…	…	…	…
	…	…	…	…	60	5.68	0.905	5.91	0.943	…	…	…	…
	…	…	…	…	80	5.52	0.762	5.73	0.792	…	…	…	…
	…	…	…	…	100	6.04	0.746	6.24	0.772	…	…	…	…
	…	…	…	…	120	7.17	0.808	7.37	0.832	…	…	…	…

Table 2
(Continued)

						Inelastic		Total		Fit			
o/p	i	f	ω	ν	T	σ_{if}	γ_{if}	σ_{if}	γ_{if}	g	a	$b \times 10^5$	c
Ortho	3	7	3977	132.7	20	6.54	1.808	11.57	3.196	1.051	758.84	3.5965	102.68
	⋯	⋯	⋯	⋯	40	5.32	1.039	8.44	1.648	⋯	⋯	⋯	⋯
	⋯	⋯	⋯	⋯	60	6.15	0.982	8.58	1.369	⋯	⋯	⋯	⋯
	⋯	⋯	⋯	⋯	80	6.32	0.873	8.39	1.159	⋯	⋯	⋯	⋯
	⋯	⋯	⋯	⋯	100	7.26	0.897	9.13	1.128	⋯	⋯	⋯	⋯
	⋯	⋯	⋯	⋯	120	8.18	0.923	9.92	1.119	⋯	⋯	⋯	⋯

Note. Units: line frequency ω in GHz, wavenumber ν in cm^{-1}, T in K, σ_{if} in $Å^2$, γ_{if} in MHz $Torr^{-1}$ (divide by 39.45 to translate into cm^{-1} atm^{-1}). Fit parameters g, a, b, c according to Equation (9).

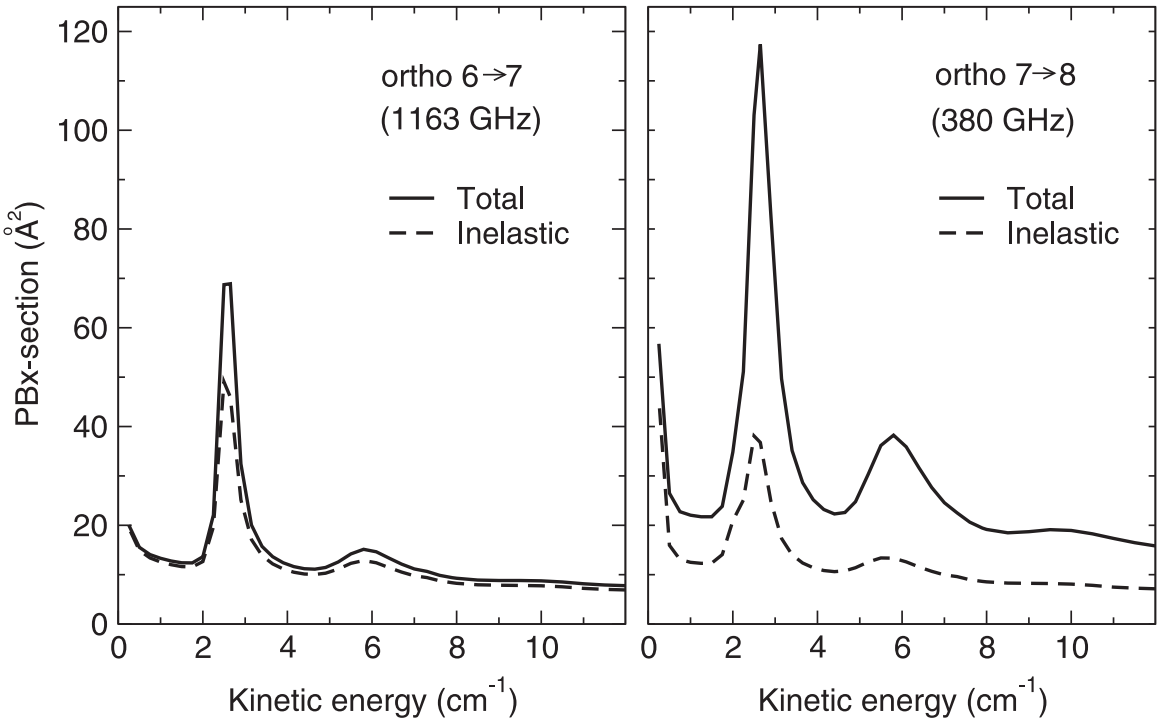

Figure 2. PBx-sections vs. kinetic energy for two rotational lines of H_2O.

The elastic contribution, in contrast, depends more specifically on the particular $i \rightarrow f$ transition. In addition, this component always increases at lower temperatures, and can be significantly large at 20 K, causing a considerable dispersion in the total PB-coefficients. The described dependence with temperature had already been observed in linear molecules (Thibault et al. 2000, 2001, 2002), where it was also noted that the elastic contribution is larger for lower values of the rotational quantum number J, in exact correlation with the rotational energy and with the line frequency. In the present case, only a coarse inverse correlation of the elastic contribution with the line frequency can be guessed, and, due to the asymmetric top character of H_2O, there is no simple relation between line frequencies and rotational energy or angular momentum. For example, the lines at 1153 and 1163 GHz are close in frequency but they show different elastic PB, while the lines at 380 and 1661 GHz, far in frequency, have similar elastic PB. This behavior is further confirmed by other lines in Table 2.

We present in Figure 2 the dependence with the kinetic energy of the total and inelastic PBx-sections for two representative lines, the $6 \rightarrow 7$ (1163 GHz) and the $7 \rightarrow 8$ (380 GHz) lines of ortho-H_2O. Both transitions exhibit some low-energy resonances (at ~2.5 and ~6 cm^{-1}), already reported as shape resonances by Dagdigian & Alexander (2010). For the $6 \rightarrow 7$ line, the elastic contribution (inspected by difference between the total and the inelastic PBx-sections) is negligible but at the resonances. On the contrary, for the $7 \rightarrow 8$ line, this contribution is significant for all energies, and increases near the resonances. Enhancement of the elastic contribution at resonances can be explained by sharp changes in the scattering amplitudes as functions of the kinetic energy. These resonances, which appear for all the transitions studied here, play an increasing role in the thermally averaged PBx-sections as temperature decreases.

Regarding the total PBx-sections, as temperature decreases most of them drop, reach a minimum at different T depending on the line, and then grow up. The exception is, again, the $1 \rightarrow 2$ (1113 GHz) line of para-H_2O, which decreases monotonically in the 120 to 20 K thermal range. Calculated total PBx-sections by Maluendes et al. (1992) for the $5 \rightarrow 6$

(183 GHz) line of para-H_2O and the $7 \rightarrow 8$ (380 GHz) line of ortho-H_2O, from 50 K to above room temperature, also show a decreasing trend with decreasing temperature, with a minimum between 50 and 100 K. However, these PBx-sections are smaller than those calculated here with the PES by Patkowski et al. (2002), as was also observed for the homologous sts-rates for inelastic collisions, as mentioned in Section 3. It should be pointed out that the PBx-section $\sigma_{if}(E_k)$ calculated by Maluendes et al. (1992) for the 183 GHz line does not show any resonance at low kinetic energy, as opposed to the present work where such resonances have been shown to contribute appreciably to the thermally averaged PBx-section $\sigma_{if}(T)$.

We switch finally to the total PB-coefficients $\gamma_{if}(T)$ between 20 and 120 K reported in Table 2. They show an almost flat trend at higher temperatures, with a shallow minimum at $80 \leqslant T \leqslant 120$ K, and then grow up markedly for $T \leqslant 40$ K. While the thermal dependence of the PB-coefficients is usually modeled by empirical power laws like

$$\gamma_{if}(T) = \gamma_{if}(T_0)\left(T/T_0\right)^{\alpha}, \tag{8}$$

assuming a monotonic dependence with T, in the present case such a simple dependence cannot be safely used because of the minima. We propose, for the PB-coefficients of H_2O lines by helium, the alternative trend-law for the $20 \leqslant T \leqslant 120$ K range

$$\gamma_{if}(T) = g + a/T^2 + b\,(T - c)^2. \tag{9}$$

The parameters g, a, b, c, given in Table 2 for each line, provide an average accuracy better than 3% for most PB-coefficients with respect to the values reported in Table 2 for discrete temperatures, allowing for a safer interpolation than by using Equation (8).

To conclude, the present study shows that the PB of H_2O spectral lines by He is a complex phenomenon, which does not seem amenable to simple relations with line frequency nor angular momentum. Special care must be paid to the elastic contribution, which is not included in the RPA, but plays a significant role here: it is eventually responsible for the observed dispersion in the total PB-coefficients, can be dominant at 20 K, and is expected to further increase at lower temperatures. The present results are thus intended as a useful guide for future laboratory measurements and astrophysical observations.

Thanks are due to B. J. Drouin and J. C. Pearson for providing their experimental data on PB-coefficients for H_2O:He collisions, and to J. L. Domenech for helpful comments on the manuscript. This work has been supported by the Spanish Ministerio de Economía y Competitividad (MINECO), grants FIS2013-48275-C2 and CONSOLIDER-ASTROMOL CSD2009-0038.

APPENDIX
CLOSE-COUPLING CALCULATIONS

In this appendix we present the details for the CC calculation with the MOLSCAT code of the PBx-section for a given electric–dipole transition, using the PES by Patkowski et al. (2002). The MOLSCAT code does not provide an option to just retrieve the elastic contribution of Equation (5). However, it allows for the calculation of the total (elastic plus inelastic) PBx-section in a straightforward manner. Therefore, we have obtained the elastic contribution as the difference

$$\sigma_{if}^{(\mathrm{el})\mathrm{CC}}(T) = \sigma_{if}^{\mathrm{CC}}(T) - \sigma_{if}^{(\mathrm{in})\mathrm{CC}}(T), \tag{10}$$

between the total PBx-section, $\sigma_{if}^{\mathrm{CC}}(T)$, and the inelastic contribution, $\sigma_{if}^{(\mathrm{in})\mathrm{CC}}(T)$.

In the equation above, $\sigma_{if}^{\mathrm{CC}}(T)$ involves a thermal average of a set of PBx-sections in terms of the kinetic energy, $\sigma_{if}^{\mathrm{CC}}(E_k)$, according to the well-known Equation (20) of Shafer & Gordon (1973). PBx-sections $\sigma_{if}^{\mathrm{CC}}(E_k)$ were computed using the hybrid log-derivative-Airy propagator by Alexander & Manolopoulos (1987) implemented in MOLSCAT, and are converged (with respect to basis set size, propagation parameters and number of partial waves) to better than 1%. The calculations were carried out for kinetic energies up to 850 cm^{-1}, taking care of using small energy steps ($\Delta E_k \leqslant 0.5\ \mathrm{cm}^{-1}$) for the lowest energies in order to describe properly the resonant structures of the cross sections. As discussed in the main text, such resonances play a relevant role in most PBx-sections at low temperature. The resulting thermally averaged $\sigma_{if}^{\mathrm{CC}}(T)$ are converged within 5% at 20 K, or better at higher temperatures.

On the other hand, the inelastic PBx-section $\sigma_{if}^{(\mathrm{in})\mathrm{CC}}(T)$ in Equation (10) can be computed either from a thermal average of the ordinary cross sections for inelastic collisions from the MOLSCAT output, or by means of Equation (4) using the sts-rates for inelastic collisions from the Patkowski PES reported by Tejeda et al. (2015; P-rates therein); we checked that both procedures yield the same result.

REFERENCES

Alexander, M. H., & Manolopoulos, D. E. 1987, JChPh, 86, 2044
Baranger, M. 1958, PhRv, 112, 855
Dagdigian, P. J., & Alexander, M. 2010, MolPh, 108, 1159
DePristo, A. E., & Rabitz, H. 1979, JQSRT, 22, 65
Dick, M. J., Drouin, B. J., & Pearson, J. C. 2010, PhRvA, 81, 022706
Drouin, B., & Wiesenfeld, L. 2012, PhRvA, 86, 022705
Dubernet, M.-L., Alexander, M. H., Ba, Y. A., et al. 2013, A&A, 553, A50
Dutta, J. M., Jones, C. R., Goyette, T. M., & de Lucia, F. C. 1993, Icar, 102, 232
Faure, A., Wiesenfeld, L., Drouin, B. J., & Tennyson, J. 2013, JQSRT, 116, 79
Goyette, T. M., & de Lucia, F. C. 1990, JMoSp, 143, 346
Green, S. 1980, JChPh, 73, 2740
Green, S. 1989, JChPh, 90, 3603
Green, S., Maluendes, S., & McLean, A. D. 1993, ApJS, 85, 181
Hutson, J. M., & Green, S. 1994, MOLSCAT Computer Code, version 14, Distributed by Collaborative Computational Project No. 6 of the UK Science and Engineering Research Council
Maluendes, S., McLean, A. D., & Green, S. 1992, JChPh, 96, 8150
Palma, A., & Green, S. 1986, JChPh, 85, 1333
Patkowski, K., Korona, T., Moszynski, R., Jeziorski, B., & Szalewicz, K. 2002, JMoSt THEOCHEM, 591, 231
Schöier, F. L., van der Tak, F. F. S., van Dishoeck, E. F., & Black, J. H. 2005, A&A, 432, 369
Shafer, R., & Gordon, R. G. 1973, JChPh, 58, 5422
Tejeda, G., Carmona-Novillo, E., Moreno, E., et al. 2015, ApJS, 216, 3
Tennyson, J., Zobov, N. F., Williamson, R., Polyansky, O. L., & Bernath, P. F. 2001, JPCRD, 30, 735
Thibault, F., Calil, B., Boissoles, J., & Launay, J. M. 2000, PCCP, 2, 5404
Thibault, F., Calil, B., Buldyreva, J., et al. 2001, PCCP, 3, 3924
Thibault, F., Fuller, E. P., Grabow, K. A., et al. 2009, JMoSp, 256, 17
Thibault, F., Martinez, R. Z., Domenech, J. L., Bermejo, D., & Bouanich, J.-P. 2002, JChPh, 117, 2523
van Dishoeck, E. F., Herbst, E., & Neufeld, D. A. 2013, ChRv, 113, 9043
van Dishoeck, E. F., Kristensen, L. E., Benz, A. O., et al. 2011, PASP, 123, 138
Wiesenfeld, L., & Faure, A. 2010, PhRvA, 82, 040702
Yang, B., Nagao, M., Satomi, W., Kimura, M., & Stancil, P. C. 2013, ApJ, 765, 77